27 Apr 1981, 2:00 pm - 5:00 pm

The Cyclic Loading Behavior of Grouted Sand

J. L. Rosenfarb
Drexel University, Philadelphia, PA

R. E. Hackman
Drexel University, Philadelphia, PA

Proceedings: First International Conference on Recent Advances in Geotechnical Earthquake Engineering and Soil Dynamics, April 26 - May 3, 1981, St. Louis, Missouri

The Cyclic Loading Behavior of Grouted Sand

J. L. Rosenfarb
Assistant Professor of Civil Engineering, Drexel University, Philadelphia, Pennsylvania

R. E. Hackman
Research Assistant, Dept. of Civil Engineering, Drexel University, Philadelphia, Pennsylvania

SYNOPSIS A two-phased static and dynamic laboratory investigation of the behavior of a silicate grout stabilized sand has been undertaken. Through the use of load-controlled cyclic triaxial testing the dynamic strength, stiffness, and deformation characteristics have been assessed as a function of mix design, confinement level and loading history. Comparisons between static and dynamic properties are provided.

INTRODUCTION

With the rapid expansion of engineered construction, it is becoming increasingly more difficult to obtain sites that are immediately suitable for their intended purposes. The underlying soils may often be too weak and compressible; and can only be used in conjunction with elaborate or uneconomical foundation systems. A second alternative, however; has been made available to the engineer as a result of laboratory and field research carried on during the last thirty years. This effort has led to the development of soil stabilization techniques, whereby site soils can essentially be improved in-situ. A variety of methods are now available to improve soil strength, modify permeability, reduce compressibility, or limit frost susceptibility.

The research endeavor, as presented herein, focuses on the general stabilization technique known as chemical grout injection and deals strictly with the silicate-based grouts which are now widely used by the various grouting contractors both in the United States and abroad. The application of this type of stabilization has been primarily directed towards the solution of problems associated with static loading conditions. Accordingly, past research has been aimed at determining the short-term static behavior of chemically grouted soils (e.g. Warner (1972); Clough, et. al (1979). These studies have provided a good background for the design and use of chemical grouts (including the silicate variety) in the many engineering applications where only static loading is relevant.

Soil stabilization using chemical grouts has also been successfully applied to soils which are subject to dynamic (or cyclic) loading conditions. For example, chemical grouts have been used to reduce excessive vibrations resulting from dynamically loaded machine foundations (Gnaedinger (1961)); to stabilize the soil beneath a railroad track structure (--(1964)); or to provide support during and after subway tunnel construction (Tan and Clough (1980)). These applications have been successful largely due to the experience of the engineers and contractors involved with the projects, and not because they conformed to any rigid design scheme. The reason for the lack of such a design methodology is due to the fact that the behavior of chemically grouted soils subjected to dynamic loading conditions is relatively unknown. A limited laboratory investigation was conducted by Shen and Smith (1976). Analysis of the test data yielded values for the conventional elastic constants as well as damping capacity for a single grout mix design. Consequently, it becomes of prime importance to understand both the short-term as well as the long-term dynamic behavior of such stabilized soils for a variety of grout mixes. Accordingly, it is this goal which serves as the basis for the work to be presented herein.

In order to accomplish this goal, a two-phased laboratory investigation was undertaken. In the first phase, a series of drained-static triaxial tests were conducted on test specimens that were prepared using a simulated grout injection system. These tests were conducted in order to assess the effectiveness and reproducibility of the injection system, as well as to obtain strength level information needed for the next phase of the investigation. This second phase consisted of subjecting the grouted specimens to drained-dynamic triaxial tests, whereby, the specimens were placed under varying levels of mean load with a deviator load being cycled sinusoidally above and below the mean.

DESCRIPTION OF EXPERIMENTAL PROGRAM

Table 1 summarizes the test variables and their ranges as investigated in both the static and dynamic phases. Sand type, grout type, and curing environment parameters were all held constant for both test phases.

Specimen Preparation

The sand used was a commercially available Ottawa sand having a mean particle diameter of 0.5 mm and a coefficient of uniformity of 1.4. A sodium silicate grout was used in this investigation. This type of grout generally consists of four components: (1) sodium silicate, as a base; (2) a catalyst (hardener); (3) a gel accelerator or an inhibitor; and (4) water. The sodium silicate component was a commercially obtained product from The Philadelphia Quartz Company and had the following composition (by weight): 9.1% Na_2O; 29.2% SiO_2; and 61.7% H_2O. This solution had a viscosity of 206 centipoise, a specific gravity of 1.401 at 20°C, and a pH of 10.5. Both the catalyst and a gel accelerating agent were obtained from a local grouting contractor. Untreated tap water at room temperature was used as the fourth grout component. Determination of component concentrations

TABLE I. Summary of Variables Investigated

Effect of	Specific variable	Range investigated
Sand characteristics	Initial density Grain size	15.4 - 15.9 kN/m^3 d_{50}=0.5mm; CU=1.4
Grout mix	Sodium silicate content Catalyst content Accelerator content Water content	30 - 45 % (by vol.) 10 % (by vol.) 10 % (by vol.) 35 - 50 % (by vol.)
Curing environment	Curing period Type of cure	7 days moist
Specimen confinement	Triaxial cell pressure	0 and 100 kN/m^2
Loading conditions (static tests)	Load rate	1.1 kN/min (load control)
Loading conditions (dynamic tests)	Mean deviator load Cyclic deviator load Waveform Loading duration	30 - 70 % of static failure load 25 - 50 % of mean deviator load 1 Hz sinusoidal variable

Note: 1 kN/m^3 = 6.36 pcf; 1 kN/m^2 = 0.15 psi; 1 kN/min = 225 lb/min

for the test program were selected as indicated in Table 2. Catalyst and gel accelerator concentrations were maintained at a constant 10% independent of the silicate contents. Although equipment limitations precluded the selection of a wider range of silicate concentrations, the 30% to 45% range, however, is typical of United States practice.

TABLE II. Component Concentrations of Grout Mixes

	Component (% by weight)			
Mix Type	Sodium Silicate	Catalyst	Accelerator	Water
I	30	10	10	50
II	40	10	10	40
III	45	10	10	35

A total of 184 specimens were manufactured using a procedure selected in order to simulate as closely as possible in situ field conditions of grout injection (Clough, et. al. (1979)). Essentially, the grout solution was forced up through a set of cylindrical tubes containing the Ottawa sand which had been placed at a predetermined density. Figure 1 shows a schematic of the grouting apparatus. The four aluminum split cylinders were filled with Ottawa sand to initial densities as given in Table 1. Water was used to first saturate the specimens under a pressure of about 6.9 kN/m^2 (1 psi). With the specimens saturated and the grout properly mixed, the supply tank was filled with the liquid grout and pressurized to 34.5 kN/m^2 (5 psi). Following the ensuing injection of the grout, the specimens were allowed to cure inside the cylinders for a period of 24 hours after which they were removed, sealed, and stored in a moist condition for seven days until testing.

Experimental Equipment and Procedures

The primary testing apparatus consisted of a servo-controlled pneumatic actuated triaxial system manufactured by Structural Behavior Engineering Laboratories (SBEL) of Phoenix, Arizona. For purposes of this investigation, all tests using the SBEL system were of the load-controlled variety with the feedback coming directly from the integral load cell located in the base of the triaxial cell as shown in Figure 2. Axial deformations were determined electronically using the cell mounted displacement transducer (LVDT). Load and displacement outputs were simultaneously recorded on an x-y recorder. Some additional strength testing was also conducted using a conventional strain-controlled triaxial system.

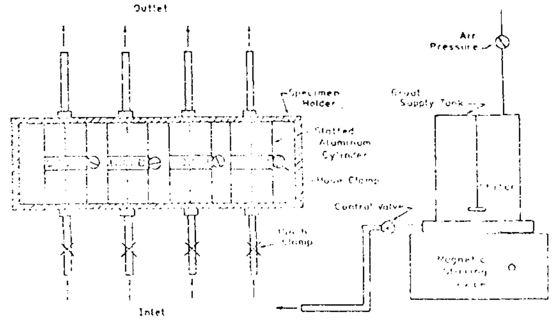

Fig. 1. Chemical Grouting Apparatus

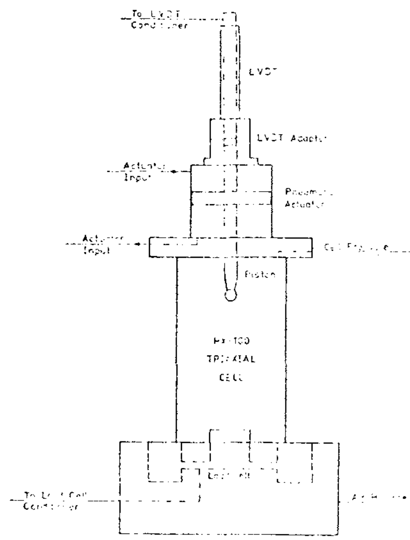

Fig. 2. Dynamic Triaxial Cell

As mentioned earlier, a series of static tests were conducted in order to assess the grouted sand strength parameters and to develop the loading program for the major dynamic testing phase. This series consisted of both a group of drained strain-controlled and drained load-controlled triaxial tests. The strain-controlled tests (strain rate of 1.7 - 2.5%/min), which were conducted using confining pressures ranging from 0 to 100 kN/m^2 (15 psi), were used primarily to evaluate the variation of the strength parameters with grout concentration. The load-controlled tests were performed using the static loading capabilities of the SBEL dynamic triaxial system. By employing a ramp waveform having a period of 60 seconds, a loading rate of 1.1 kN/min (250 lb/min) was established. Drained strength and stiffness was evaluated for samples placed under confining pressures of 0 and 100 kN/m^2 (0 and 15 psi). For both these series as well as the dynamic tests, which will be discussed subsequently, the ends of the grouted specimens were carefully ground on a lapidarian wheel in order to insure proper specimen seating. After determining the initial length, diameter, and weight, specimens were placed on the lucite bottom platen of the triaxial cell. A standard thin latex membrane was used to encase the specimen and the drainage lines were connected to the upper and lower platens which contained porous stone inserts. For tests employing confining pressure, shearing was initiated almost immediately with very little consolidation time allocated (i.e., 5 to 10 min. maximum).

All dynamic testing was conducted using the SBEL dynamic triaxial system. Two types of tests were included in this phase of the experimental program. The first type consisted of loading the specimen in increments or stages. For each stage an initial or mean axial compressive load, q_m, was applied to the specimen. Once this load was established, a compressive load component, q_c, was cycled above and below the mean load. The mean load varied from 30 to 70 percent of the specimen's static strength as determined from the load controlled static tests. The cycled component was set at either 25 or 50 percent of the mean load value. This pattern of loading characterized the staged dynamic tests. Each stage consisted of approximately 1000 loading/unloading cycles using a sinusoidal waveform with a frequency of 1 Hz. This staged pattern of loading was continued until the specimen failed. During this process, load-deformation data was output to an x-y recorder and permanent traces were usually obtained after 10, 50, 100, 250, 500, and 1000 cycles of loading.

The second type of dynamic tests consisted of loading the specimen to a predetermined mean load level, applying a cyclic load and then allowing the cycling of the load to continue until the specimen failed. This pattern of loading characterized the continuous dynamic test. Again, a sinusoidal waveform was used with a frequency of 1 Hz. Information obtained from the staged loading tests was always used to select loading parameters for the continuous tests. In particular, the stage before failure was usually chosen for the single loading cyclic test. This type of test was developed as an attempt to define whether failure in the stage loading test was due to the increase in the maximum cyclic load level or to the number of cycles completed for the previous stages. Load-deformation data was recorded during the prefailure period as previously described.

In summary, each batch of grouted sand samples consisted of four specimens having the same sodium silicate content. One specimen was tested statically using a relatively fast loading rate; another specimen was tested statically using a much slower loading rate; the third specimen was tested dynamically using a multi-staged loading procedure; and the fourth specimen was also tested dynamically using a single stage loading procedure.

PRESENTATION OF RESULTS

Static Behavior

Figures 3 and 4 show typical stress-strain reponses for specimens tested under confined and unconfined conditions, respectively. The effect of sodium silicate concentration on load-controlled static strength is illustrated in Figure 5. The general static behavior is such that as the silicate content of the grout increases, the peak static strength of the grouted sand also increases. Clearly, the effect of confinement is to increase the strength of the grouted sand at each particular silicate content.

Secant moduli (defined as the slope of the secant line drawn from the point of initial loading to a point equal to 50 percent of the peak load) varied from 20,000 to 60,000 kN/m^2 (3000 to 9000 psi) for the unconfined tests and from 50,000 to 130,000 kN/m^2 (7500 to 19,500 psi) for the confined tests. The general behavior of the grouted sand is such that the secant modulus increases in value as the silicate content of the grout increases.

Finally, axial strains at failure were relatively unchanged by variations in sodium silicate content and averaged about 1.5% for the case of no confinement. For the confined tests, however, failure strains decreased with increasing percentages of sodium silicate and

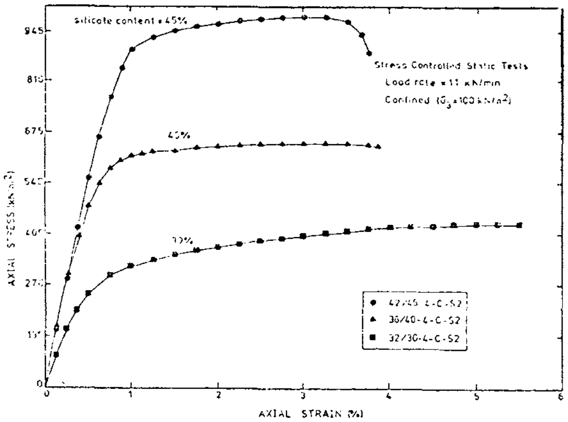

Fig. 3. Static Stress-Strain Response (Confined)

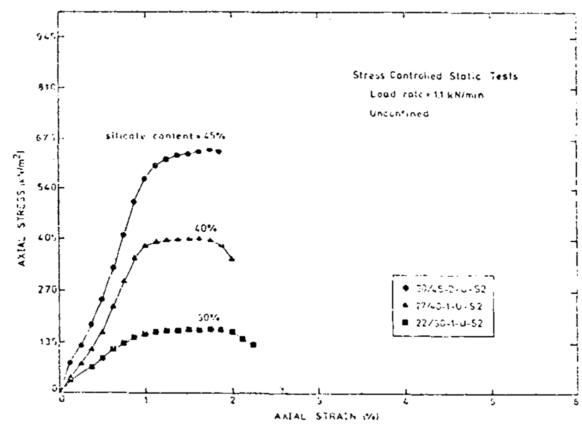

Fig. 4. Static Stress-Strain Response (Unconfined)

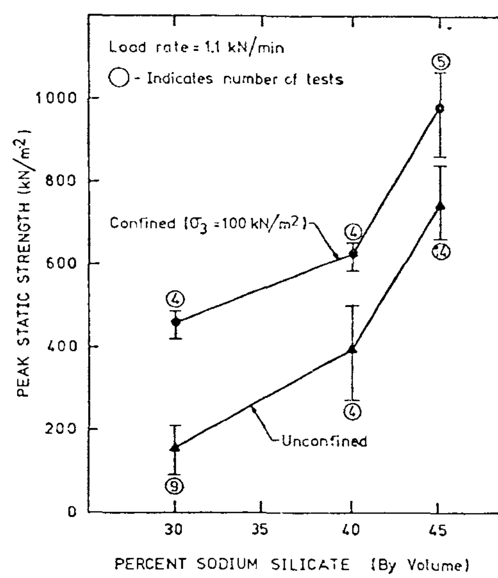

Fig. 5. Variation of Peak Static Strength

ranged from 5% (for 30% silicate) to 3% (for 45% silicate).

The behavior as summarized above for the strength, moduli, and axial strain exhibited by the specimens in this program was consistent with results as previously reported (e.g. Warner (1972); Clough, et. al. (1979)). This agreement served as a validation of the sample preparation procedure as used herein.

Dynamic Behavior

The analysis of the dynamic behavior of grouted sand was based primarily upon the stress-strain loops that were recorded as the testing progressed. A typical loop is shown in Figure 6. The strength, stiffness, and strain behavior, as discussed in subsequent sections, were determined from analyzing the series of loops for a given test and then synthesizing the resulting data to provide an indication of the dynamic behavior of silicate-grouted sand.

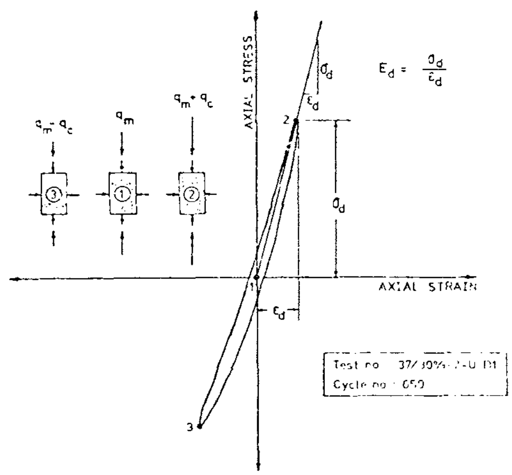

Fig. 6. Typical Dynamic Stress-Strain Loop

The general strength behavior when subjected to cyclic loading conditions was such that the strengths of the specimens increased with increasing percentages of sodium silicate (as in the static case). Based on the results of this investigation, cyclically loaded specimens failed at lower strength values than the statically loaded specimens. The dynamic strengths ranged from 74 to 567 kN/m^2 (11 to 86 psi) for the unconfined stage loading tests, and from 378 to 793 kN/m^2 (57 to 119 psi) for the confined stage loading tests. The corresponding strength values for the continuous loading tests ranged from 91 to 544 kN/m^2 (14 to 82 psi) and from 412 to 649 kN/m^2 (62 to 112 psi). Figure 7 shows a comparison between static and dynamic strengths. Plotted against silicate content is the strength ratio, SR, defined as the ratio of dynamic to static strengths. For purposes of comparison, the specimens used in the static tests were obtained from the same batch (group of four units) as those in the dynamic tests. In all cases, the dynamic strengths were less than the static strengths with this behavior most pronounced for the unconfined tests. For this series, the effect of increasing silicate content was to increase the strength ratio, while for the confined series an opposite trend was apparent. Based on these results it would appear as if a common strength ratio would be achieved given higher silicate contents than tested. Despite the number of tests conducted, no definitive conclusions, however, can be made with respect to the influence of load history (i.e. staged or continuous testing) on the strength ratio.

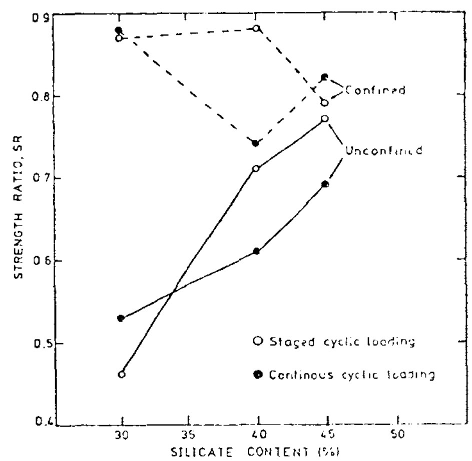

Fig. 7. Variation of Strength Ratio, SR

A stiffness or dynamic Young's modulus E_d, was defined as indicated in Figure 6. The general behavior was such that the stiffness modulus increased with increasing percentages of sodium silicate. In addition, moduli attained peak values before beginning to decrease as the specimens tended toward failure. The variation of the stiffness modulus with silicate content for the various stages of loading can be seen in Figures 8 and 9, for the unconfined and confined cases, respectively. Values ranged from about 80,000 to 320,000 kN/m^2 (12,000 to 48,000 psi) for no confinement; and from 200,000 to 360,000 kN/m^2 (30,000 to 54,000 psi) with confinement. In Figure 8 large increases in modulus are exhibited for increasing silicate content; whereas, in Figure 9 relatively small increases are apparent. Such a behavior would seem to indicate that the beneficial effect of increasing silicate content on the dynamic stiffness modulus is reduced as the level of confinement is increased. In terms of stress (or strain) history, it can be seen that the moduli in both Figures 8 and 9 exhibit an increasing trend until the third stage of loading; then a decreasing trend until failure occurs. This work hardening/softening type of behavior seems to be independent of the silicate content of the grout.

To analyze the stiffness behavior for silicate-grouted sands subjected to continuous-loaded dynamic tests, a modulus ratio, MR, was defined as the ratio of the dynamic modulus, E_d, to the static modulus, E_s. The static modulus was defined as the secant modulus taken at 50 percent of the mean load level (qm) for the static loading portion of the continuous test. This ratio can then be investigated in three areas of the continuous test: (1) the initial ratio (using the E_d for the 10th cycle), (2) the peak ratio (using the maximum E_d obtained during testing), and (3) the final ratio (using the E_d for the cycle immediately before failure). The dynamic moduli ranged from 3.4 to 7.9 times greater than the static moduli for the unconfined case, and from 2.5 to 4.0 times greater for the confined case as indicated in Figure 10. Again, this behavior seems to indicate that the effect of confinement is to reduce the peak modulus ratio.

The behavior exhibited by the ratio for the unconfined case (Figure 10a) is characterized by an increasing trend for increases in the silicate content. However, the behavior for the confined case (Figure 10b) shows a decrease in the ratio in the 30 to 40 percent range followed by an increase in the 40 to 45 percent range. Further testing would be required to verify these trends.

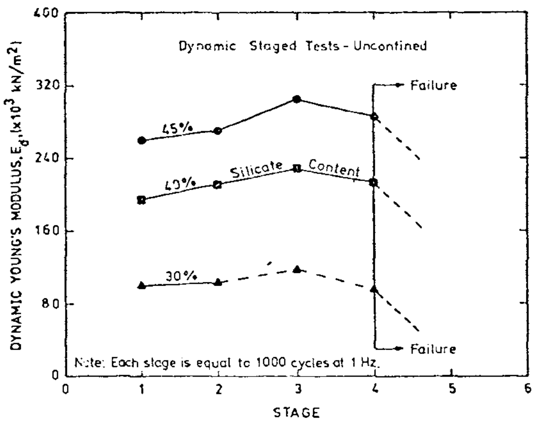

Fig. 8. Dynamic Young's Moduli for Unconfined Staged Tests

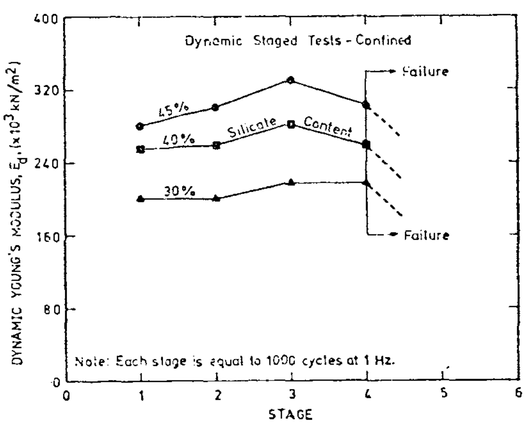

Fig. 9. Dynamic Young's Moduli for Staged Confined Tests

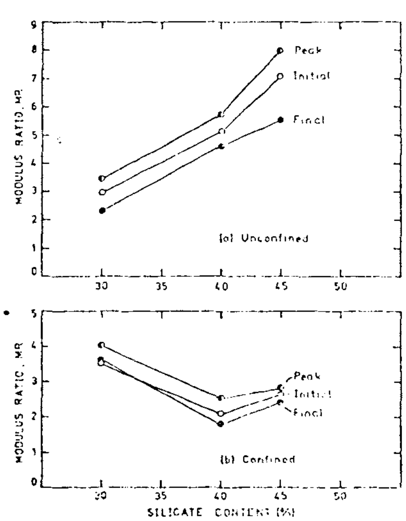

Fig. 10. Variation of Modulus Ratio, MR for Continuous Tests

The general axial strain behavior of silicate-grouted sands as determined from this investigation was characterized by a reduction of strain at failure with increasing levels of silicate content for the condition of confinement. On the other hand, for the unconfined tests, little or no change in the axial failure strain as a function of silicate content was evidenced. The dynamic strain behavior at failure as a function of silicate content for the dynamic stage tests is shown in Figure 11 which presents averaged data for the unconfined and confined cases. In the unconfined tests, there was very little variation of the strain values at failure (1.4% to 1.7%) while in the confined tests there was a sharp decrease in strain level as the silicate content was increased, thus indicating a much more pronounced brittle type of behavior (4% to 8%).

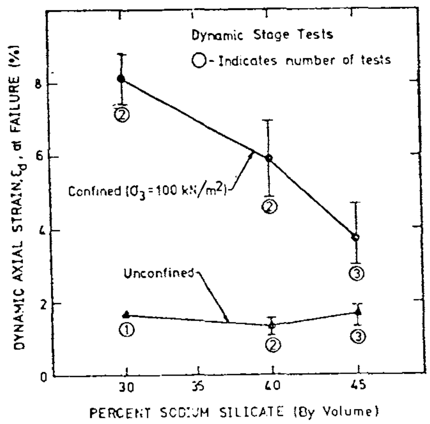

Fig. 11. Variation of Dynamic Failure Strains for Staged Tests

The continuous test involves only one static axial strain component which results from the application of of the mean load level (q_m) at the beginning of the test; and the remaining axial strain is developed from the number of loading cycles imposed upon the specimen. Figure 12 shows the typical development of dynamic axial strain as a function of the number of loading cycles for the case of unconfined, 45% silicate specimens. As shown in Figure 13, the failure strain behavior closely parallelled that observed for the staged tests. Values ranged from 1.4% to 2.2% for the unconfined tests, and 4% to 10% for the confined tests.

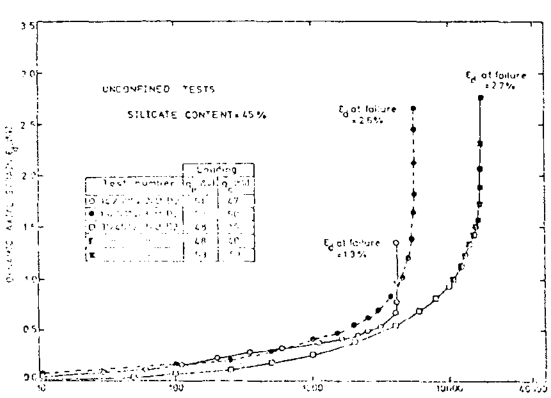

Fig. 12. Typical Dynamic Strain Behavior for Continuous Test

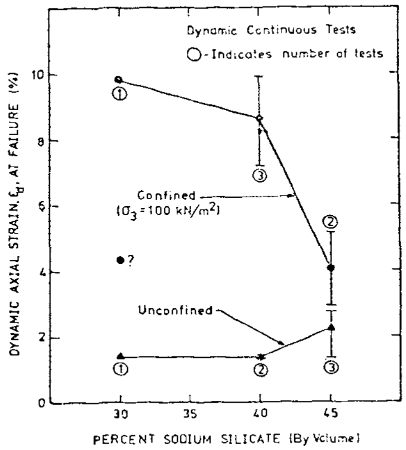

Fig. 13. Variation of Dynamic Failure Strains for Continuous Tests

Differences in the failure strain behavior associated with specimens tested under confinement as compared to those tested under no confinement were determined as mentioned previously. In an effort to further quantify this behavior, specimen durability was assessed through calculations of cummulative internal strain energy as summarized in Table 3. Specifically, the static component during a dynamic test, W_s, was defined as

$$W_s = \Sigma[\sigma_m(i)\epsilon_m(i)] \quad (1)$$

where $\sigma_m(i)$ is the mean stress during stage i and $\epsilon_m(i)$ is the axial strain associated with the application of the mean stress $\sigma_m(i)$. The corresponding dynamic component, W_d, was defined as

$$W_d = \Sigma[\sigma_c(i)\epsilon_c(i)] \quad (2)$$

where $\sigma_c(i)$ is the maximum cyclic stress during stage i and $\epsilon_c(i)$ is the axial strain associated with the application of the cyclic stress $\sigma_c(i)$. For purposes of comparison, the strain energy dissipated in a load-controlled static test specimen $\bar{W}_s$, was also computed as the area under the associated stress-strain curve.

TABLE III. Summary of Cummulative Specimen Strain Energy in $(kN/m^2)/(cm/cm)$

	Silicate Content	Static Strain W_s	Dynamic Staged			Dynamic Continuous		
			Static Component W_s	Dynamic Component W_d	Total W	Static Component W_s	Dynamic Component W_d	Total W
Unconfined	30%	2.3	0.1	1.1	1.2	0.1	1.3	1.4
	40%	4.1	0.3	3.7	4.0	0.6	3.9	4.5
	45%	7.0	0.5	7.8	8.3	1.2	14.0	15.2
Confined	30%	22.7	0.2	26.0	27.0	0.5	40.8	41.3
	40%	24.1	0.5	30.5	31.0	0.6	44.1	44.7
	45%	24.8	1.6	26.6	27.7	1.0	27.6	28.6

Based on these calculations, the effect of confinement is to increase the cummulative strain energy or in effect, the durability of the specimen. This behavior was essentially the same independent of whether the specimen was loaded statically or dynamically. In terms of silicate content, a clear increase in cummulative strain energy with increasing silicate content was only apparent for the unconfined cases. A consistent trend for the confined tests was not in evidence, most likely due to insufficient data. Finally, indicated in Table 3, the static components, W_s, associated with dynamic testing were considerably smaller than the dynamic components, W_d. Although a proper evaluation of the strain energy parameter would require a larger program of testing, there appears to be some possible correlations with the conclusions as derived earlier.

CONCLUSIONS

Based on the analysis of the data derived during this investigation, the following conclusions can be made:

1. Similar to static behavior, dynamic strengths increased with increasing sodium silicate content and confining pressure. In all cases the dynamic strengths were less than the static strengths, with this behavior more pronounced for unconfined conditions. No consistent trends were observable for changes in applied load history prior to failure.

2. Dynamic moduli increased with increasing sodium silicate content and confining pressure. The beneficial effect of increasing silicate content however, was reduced as the level of confinement was increased. Independent of applied load history, moduli attained peak values prior to beginning to decrease as failure was approached.

3. For conditions of confinement, dynamic axial strains at failure decreased as sodium silicate contents increased. Little or no variation in strain behavior as a function of silicate content was observed for the unconfined tests. Both trends were essentially independent of the type of loading history applied prior to failure; although the creep potential of silicate grouted sands should not be overlooked when interpreting long-term cyclic behavior.

4. The use of a strain energy parameter seemed to be appropriate in quantifying the effects of both silicate content and confinement on grouted sand durability.

REFERENCES

-- (1964), "Chemical Grout Licks Tough Quicksand Problem," Railway Track and Structures, February, pp. 20-22.

Clough, G. W., W. M. Kuck and G. Kasali (1979), "Silicate-Stabilized Sands," Proc., J. Geotechnical Engineering Division, American Society of Civil Engineers, Vol. 105, No. GT1, pp. 65-82.

Gnaedinger, J. P. (1961), "Grouting to Prevent Vibration of Machinery Foundations," Proc. J. Soil Mechanics and Foundations Division, American Society of Civil Engineers, Vol. 87, No. SM2, pp. 43-54.

Shen, C. K. and S. S. Smith (1976), "Elastic and Viscoelastic Behavior of a Chemically Stabilized Sand," Transportation Research Board, #593, p. 41-45.

Tan, D. Y. and G. W. Clough (1980), "Ground Control for Shallow Tunnels by Soil Grouting," Proc. J. Geotechnical Engineering Division, American Society of Civil Engineers, Vol. 106, No. GT9, pp. 1037-1057.

Warner, J. (1972), "Strength Properties of Chemically Solidified Soils," Proc., J. Soil Mechanics and Foundations Division, American Society of Civil Engineers, Vol. 98, No. SM11, pp. 1163-1186.